Heliyon 10 (2024) e23176

Contents lists available at ScienceDirect

Heliyon

journal homepage: www.cell.com/heliyon

# Remineralization effects of enamel binding peptide, WGNYAYK, on enamel subsurface demineralization *in vitro*

Yoshihito Miyayoshi, Hidenori Hamba, Keiki Nakamura, Hisako Ishizuka, Takashi Muramatsu *

*Department of Operative Dentistry, Cariology and Pulp Biology, Tokyo Dental College, 2-9-18, Kandamisaki-cho, Chiyoda-ku, Tokyo 101-0061, Japan*

ARTICLE INFO

*Keywords:*
Biomineralization
Early enamel caries
Subsurface lesion
Peptide

ABSTRACT

**Objectives:** We investigated remineralization effects of enamel binding peptide (EBP), WGNYAYK, on enamel subsurface demineralization *in vitro*.

**Methods:** Bovine lower incisor crowns were used as subsurface enamel demineralization samples, and changes of EBP binding, remineraliztion rate, hardness and microstructure were investigated. Binding of EBP, remineralization rate, hardness and structural changes were investigated. Fluorescein isothiocyatate (FITC)-labeled EBPs (0.4 mM, 4.0 mM, and 7.0 mM) were applied to the samples for 30 min at 37 °C, with sample surfaces and cross-sections observed by confocal laser scanning microscope (CLSM). Mineralization analysis samples were divided into 4 experimental groups; distilled water (DW), EBP 0.4 mM, EBP 4.0 mM, and EBP 7.0 mM. Mineral density changes were measured by micro-CT with hardness measured by nano-indentation. Samples were also observed by scanning electron microscope (SEM) for surface and longitudinal microstructure.

*Results:* CLSM images indicated that increased fluorescence was observed in the surface layer and up to about 20 μm below the surface layer. The remineralization rate was significantly higher for EBP 7.0 mM compared to DW ($p = 0.008$). Enamel surface hardness was significantly higher in all EBP groups compared to DW ($p < 0.05$) and was highest in the 7.0 mM group. SEM images showed obscuring of the superficial columnar structure in the 7.0 mM EBP group, indicating subsurface crystalline structure recovery.

*Conclusion:* The results of this study suggest that EBP binds to demineralized enamel and promotes remineralization.

## 1. Introduction

Early enamel caries is characterized by subsurface demineralization while the enamel surface is continuous and carious fossae are not yet formed. Subsurface lesions are an early stage of dental caries in which an imbalance between demineralization and remineralization exists, characterized by the acid-induced dissolution of calcium ions ($Ca^{2+}$) and phosphate ions ($PO_4^{3-}$) from subsurface enamel [1,2]. Recovery from this is induced by remineralization, in which $Ca^{2+}$ and $PO_4^{3-}$ from saliva are supplied to these lesions, promoting ion deposition in the demineralized enamel crystalline voids [3]. For this reason, a method to detect remineralization and

* Corresponding author.
*E-mail address:* tmuramat@tdc.ac.jp (T. Muramatsu).

https://doi.org/10.1016/j.heliyon.2023.e23176
Received 9 April 2023; Received in revised form 24 November 2023; Accepted 28 November 2023
Available online 1 December 2023

manage early-stage caries (remineralization therapy) is advocated [4], with the minimal intervention dentistry issued by the FDI World Dental Federation in 2016 [5]. Typical treatments include the application of remineralization-promoting substances such as fluoride, casein phosphopeptide-amorphous calcium phosphate, and nano-hydroxyapatite [6]. Fluoride interrupts the demineralization process and promotes the remineralization of enamel. These properties of fluorides are still used approaches by adding fluoride, for example to increase the hardness of the remineralized enamel. However, there are risk factors such as fluorosis associated with too frequent fluoride intakes in children under 6 years of age [7], and alternative materials have been developed.

Biomimetic enamel remineralization attracts attention [8] as a novel approach to treating and preventing early enamel caries by mimicking natural remineralization processes. Biomimetic remineralization is guided by substances that provide a scaffold for hydroxyapatite crystals to nucleate and grow, generating enamel-like structures [9]. The mineral crystals in carious lesions that is regenerated by fluoride are disordered, but biomimetic enamel remineralization induces mineral deposition and promotes oriented crystal regeneration. As biomimetic materials, amelogenin, peptides, and calcium phosphate nanoparticles are listed [10]. These specific substances include enamel matrix proteins such as enamel matrix derivative (EMD) [11] and peptides such as P11-4, a self-assembling peptide, and amelogenin-derived peptides [12,13], previously shown to remineralize enamel [11,12]. Polyamidoamine (PAMAM) dendrimers, another type of artificial protein, function well for enamel subsurface remineralization [14]. The use of proteins and protein-like molecules is often ineffective, possibly due to the inability of large molecular-weight species to penetrate the tooth subsurface. Indeed, salivary phosphoproteins such as statherin, proline-rich proteins, and histatin inhibit calcium phosphate crystal nucleation and apatite surface precipitation by enamel surface absorption [15]. On the other hand, peptides are biocompatible, specific properties are easily designed, and are more able to permeate than large proteins [16]. Phage display is one method to identify peptides with specific functions [17]. A large random library of peptides with the same number of amino acids is used in this method, identifying sequences that bind strongly to inorganic surfaces. Using this method, the 7 amino acid peptide, WGNYAYK, was identified as the enamel binding peptide (EBP) from a linear peptide library [18]. The *in vitro* study demonstrated that EBP precipitated amorphous calcium phosphate (ACP) particles from a remineralization solution containing $Ca^{2+}$ and $PO_4^{3-}$, implying involvement in calcium phosphate crystal growth [18]. However, it remains unclear whether EBPs induce the remineralization of enamel subsurface demineralization. We hypothesize that EBPs bind to demineralized enamel and promote remineralization.

In this study, we investigate the binding and remineralization properties of EBPs using demineralized enamel subsurface samples that mimic early enamel caries.

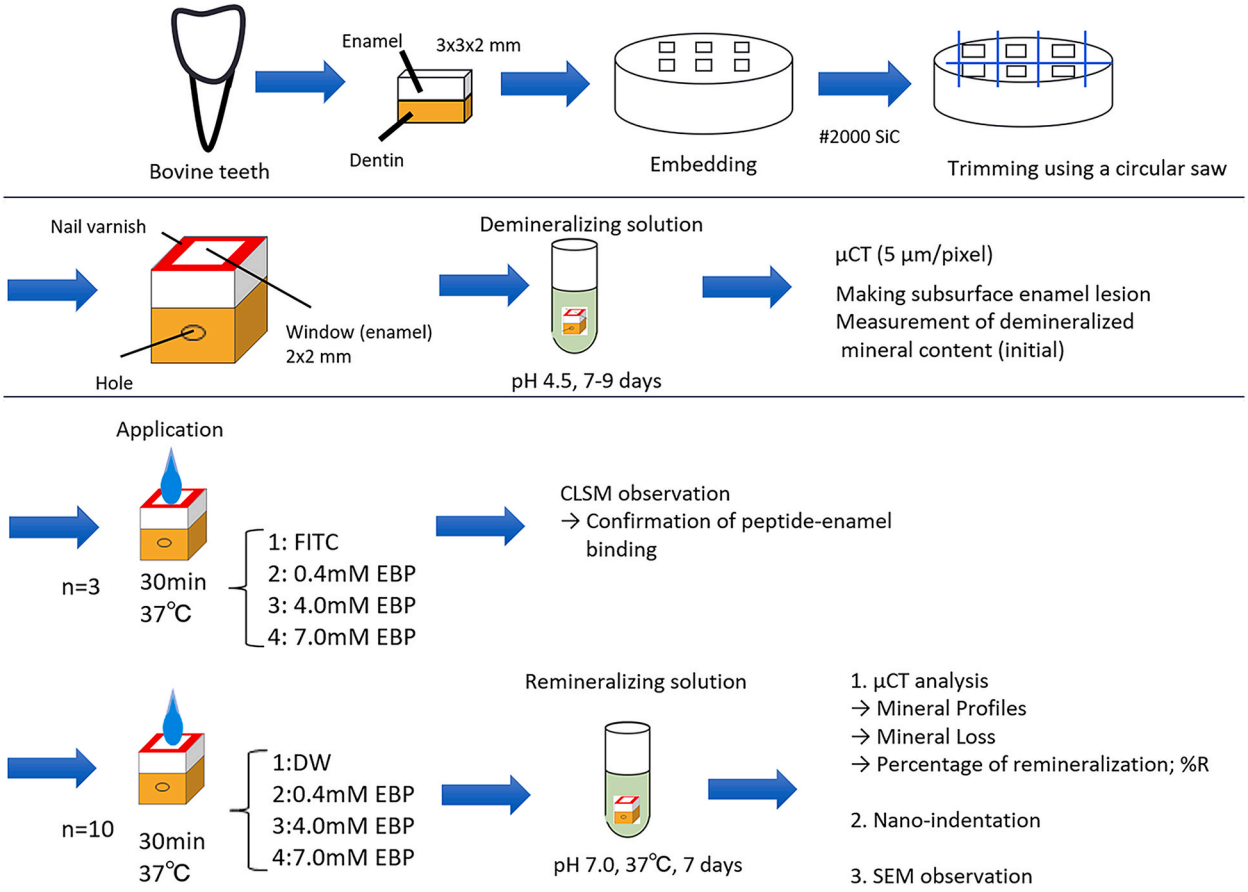


**Fig. 1.** Flow chart of the experimental design in the study.

## 2. Materials and methods

### 2.1. 2-1. Peptide preparation

Fluorescein isothiocyatate (FITC)-labeled enamel-specific binding peptide (EBP; amino acid sequence: WGNYAYK) was designed and purchased from BEX (Tokyo, Japan). Lyophilized peptide was dissolved in distilled water (DW) at 10 mg/mL to prepare EBP solutions at concentrations of 0.4 mM, 4.0 mM, and 7.0 mM [18].

### 2.2. 2-2. Enamel sample preparation

The method flowchart is shown in Fig. 1, according to the method by Ishizuka et al. (2022) with modification [19]. Thirty bovine incisors free of visible dental caries and cracks were frozen and preserved after extraction, purchased from Yokohama Meat Corporation. (Yokohama, Japan). The incisors were washed under running water to remove all adherent soft tissue. The crowns were cut to 3 x 3 × 2 mm using a precision low-speed cutting machine (Isomet, Buehler, Lake Bluff, IL, USA) and embedded into epoxy resin (EpoxiCure 2, Buehler, Lake Bluff, IL, USA). with the smooth enamel surface exposed. The enamel surface was then ground with 600–2000 water-resistant abrasive paper and ultrasonically cleaned for 5 min. The edge (1 mm) of the surface was coated with nail varnish (Revlon Red 680; Revlon, New York, NY, USA) and an observation window (2 × 2 mm) was created by exposing the polished enamel surface of each specimen [20]. Holes (1.0 mm in diameter and 0.5 mm in depth) were drilled on the side of each sample with a diamond-pointed bur for analytical alignment [21]. The prepared samples were randomly divided into the DW group, 0.4 mM EBP group, 4.0 mM EBP group, and 7.0 mM EBP group (n = 10 each). In addition, untreated enamel and demineralized enamel were added to the experimental group after 1 week of remineralization for hardness testing.

### 2.3. 2-3. Subsurface demineralization sample preparation

Subsurface demineralized lesions were prepared by immersion in demineralization solution (50 mM acetic acid, 2.2 mM $Ca(NO_3)_2$, 2.2 mM $KH_2PO_4$, 5.0 mM $NaN_3$, and 0.5 ppm NaF, pH 4.5) at 37 °C for 7–9 days to align the region depths [22,23]. In this study, mineral recovery is determined from mineral loss, which is different from demineralized depth, and is not affected by demineralized period.

### 2.4. 2-4. Confocal laser scanning microscope (CLSM)

Samples were prepared separately from the experimental group. To the treated surface was added 10 μL of the FITC-labeled EBP solution, adjusted to each concentration, and allowed to react for 30 min at 37 °C, then rinsed and dried. As a control group, 0.4 mM FITC was applied under the same conditions. To confirm enamel binding, some sample surfaces were evaluated by confocal laser microscope (LSM 880 Airy NLO, Zeiss, Jena, Germany). The samples were then cut longitudinally in the center with nippers and polished with water-resistant abrasive paper, then the longitudinal sections were evaluated. We used 3 teeth for each group, and evaluated 3 surfaces and 3 longitudinal regions.

### 2.5. 2-5. Micro-computed tomography (micro-CT)

Demineralized specimens were imaged using a micro-CT system (SMX-100CT, Shimadzu, Kyoto, Japan) at a tube voltage of 70 μA and a current of 100 kV. The subsurface region depth of each specimen was confirmed by micro-CT. The X-ray beam was oriented perpendicular to the enamel surface. To prevent drying during imaging, specimens were placed in plastic tubes and secured with a damp wipe at the top. A brass plate 0.2 mm thick was placed in the irradiation path to block low-energy X-rays and reduce line beam hardening [24].

Data were reconstructed into 3D images with a resolution of 1024 x 1024 pixels and a voxel size of 5.0 μm. A reference phantom was also scanned for calibration and included three hydroxyapatite (HAp) disks (TRI/3D-BON, Ratoc, Tokyo, Japan); two with different concentrations (0.50 and 0.70 gHAp/$cm^3$) of HAp crystals mixed with epoxy resin (Epoxicure Resin, Buehler) and one pure HAp disk (3.16 gHAp/$cm^3$) (Cellyard, Hoya, Tokyo, Japan). Enamel specimens with mean thickness of 1194 ± 96.7 μm were selected.

### 2.6. 2-6. Mineral increase rate by remineralization

Each sample was immersed in remineralization solution (0.9 mM $KH_2PO_4$, 1.5 mM $CaCl_2$, 130 mM KCl, and 1.0 mM $NaN_3$, 20 mM HEPES pH 7.0) at 37 °C for 7 days [19]. This solution was changed daily [25]. After remineralization, specimens were photographed with a micro-CT system (SMX-100CT, Shimadzu). 3D evaluation software (TRI/3D-BON, Ratoc, Tokyo, Japan) was used to align the mineral density profile by referring to the outer surface and reference hole of the CT data after demineralization and remineralization, and the mineral density profile was measured. Assuming the mineral density of the untreated enamel around the treated surface to be 100 %, the amount of mineral decreased after demineralization (ΔZd) and remineralization (ΔZr) was determined, from which the mineral change was calculated and divided by the mineral decrease after demineralization (ΔZd), from which the rate of mineral increase (%R) was obtained.

$$\%R = [(\Delta Zd\text{-}\Delta Zr) / \Delta Zd \times 100]$$

### 2.7. 2-7. Hardness test

In addition to the experimental group after 1 week of remineralization, untreated enamel and demineralized enamel were subjected to surface hardness testing using Nano-indentation (ENT-1100a, ELIONIX, Tokyo, Japan) (n = 6 each). Specimens were adjusted to a thickness of 2 mm, fixed to the stage with instant adhesive, and hardness ($N/mm^2$) was measured with a test load of 20 mN. Twenty indentations were formed in the center of each specimen [26]. The fused silica was measured and calibrated before each test for reference. Enamel specimens with mean of the sound area hardness of 33256 ± 5625.8 $N/mm^2$ were selected.

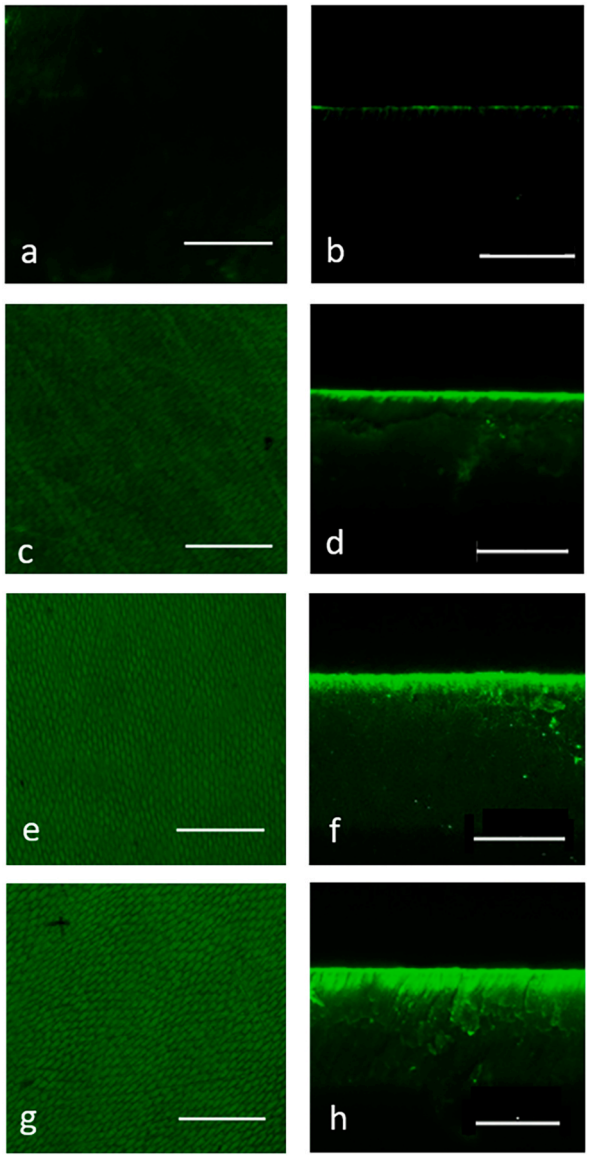


**Fig. 2.** CLSM observation of surface (I) and cross sections (II) FITC-labeled EBP fluorescence intensity increased in the superficial and cross sections compared to the control (FITC).
In the surface observation (I), EBP showed an increase in fluorescence intensity compared to the control (a). EBP 0.4 mM group (**c**) showed lower fluorescent intensity compared to the 4.0 mM (e) and 7.0 mM (g) groups. Fluorescence indicating EBP was observed in the 4.0 mM (e) and 7.0 mM (g) groups throughout the surface layer covering the enamel rod area and inter-rod enamel area
In the longitudinal section (II), increased fluorescence was observed in the surface layer and up to about 20 μm below the surface layer. An increase in fluorescence intensity was confirmed for all EBP (d, f and h) concentrations compared to the control DW (b).

### 2.8. 2-8. Scanning electron microscope (SEM)

A portion of the remineralized specimen was deposited with carbon, and the surface layer and longitudinal section microstructure was observed with a scanning electron microscope (SEM, SU-6600, Hitachi, Tokyo, Japan). The longitudinal samples were prepared in the same manner as the CLSM samples. The surface layer was observed at 7,000x magnification and the longitudinal section at 2,000x magnification (n = 3 each).

### 2.9. 2-9. Statistical analysis

All data were statistically tested for Kolmogorov–Smirnov test and the Levine's test was
applied to test for equal variance between the groups, and processed by One-way anova with.
Welch's correction and post hoc comparison by the Games-Howell test a 5 % significance level. All statistics and measure of effect size and power were performed in a statistical program.
(SPSS Version 27 for Windows, SPSS, Chicago, IL, USA).

## 3. Results

### 3.1. CLSM findings

In the surface observation (I), EBP showed an increase in fluorescence intensity compared to the control (Fig. 2a). EBP 0.4 mM group (Fig. 2c) showed lower fluorescent intensity compared to the 4.0 mM (Fig. 2e) and 7.0 mM (Fig. 2g) groups. Fluorescence indicating EBP was observed in the 4.0 mM (Fig. 2e) and 7.0 mM (Fig. 2g) groups throughout the surface layer covering the enamel rod area and inter-rod enamel area.

In the longitudinal section (II), increased fluorescence was observed in the surface layer and up to about 20 μm below the surface

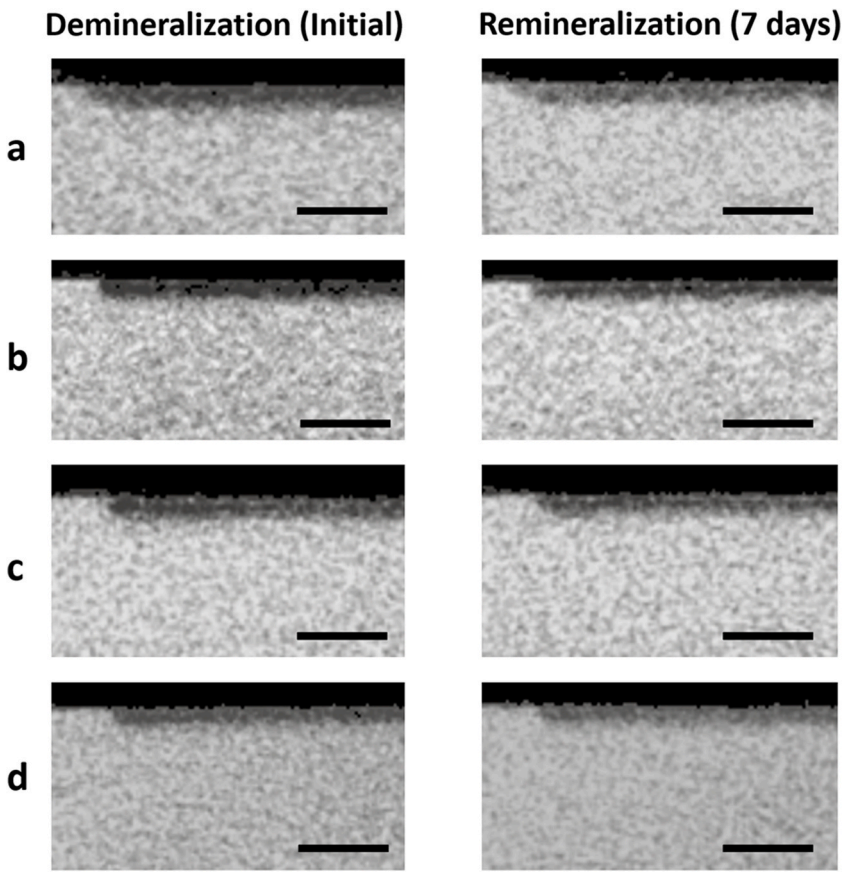


**Fig. 3.** Two-dimensional micro-focus X-ray computed tomography (micro-CT) images of the same specimens. X-ray transmission image showing enamel subsurface lesions after demineralization.
In all groups, the radiopacity increased post-remineralization (a, b, c, d).
(a) DW, (b) EBP 0.4 mM, (c) EBP 4.0 mM and (d) EBP 7.0 mM. Bars = 500 μm.

layer. An increase in fluorescence intensity was confirmed for all EBP (Fig. 2d, **f** and **2h**) concentrations compared to the control DW (Fig. 2b). Representative CLSM images are shown in Fig. 2.

### 3.2. Micro-CT and remineralization rate

In all groups, subsurface demineralization was observed, in which the most superficial layer showed a white lineation and an increase in the underlying layer permeability. In addition, an increase in radiopaque opacity of the demineralized area was observed in the micro-CT image on the 7th day of remineralization. Representative 2D images of the micro-CT are shown in Fig. 3. In all groups, the radiopacity increased post-remineralization (Fig. 3a, b, 3c and **3d)**. Representative 3D images of the micro-CT are shown in Fig. 4. X-ray transmission image showing enamel subsurface lesions after demineralization (Fig. 4a).

The radiopacity increased post-remineralization (Fig. 4b).

The mineral profiles of each experimental group are shown in Fig. 5. There was a decrease in mineral density at approximately 30 μm below the surface compared to the surface, resembling the subsurface demineralization characteristic of early caries. In all groups, a mineral density increase was observed after one week of immersion in the remineralization solution(Fig. 5a, **b**, **5c** and **5d**).

The remineralization rates are shown in Table 1. The calculated effect size was 0.259 and the power achieved was 0.815. There was no significant difference in the recalcification rate among the DW, 0.4 mM, and 4.0 mM groups, and among the 0.4 mM, 4.0 mM, and 7.0 mM groups, but there was a significant difference between DW and 7.0 mM ($p = 0.008$).

#### 3.2.1. Hardness changes in remineralized enamel after EBP application

Nano-indentation results are shown in Table 2. The unimpaired enamel showed the highest values, while the demineralized enamel showed the lowest ones. The hardness in the DW group was significantly lower than that in the demineralized group ($p < 0.001$), and in all EBP groups ($p < 0.05$). The hardness in the EBP 0.4 mM and 4.0 mM groups did not differ significantly($p = 1.00$), and the 7.0 mM group showed the highest hardness. However, the hardness in the EBP 7.0 mM group did not recover to the level of unimpaired enamel.

SEM observation.

Representative SEM images are shown in Fig. 6. Unimpaired enamel surface was smooth with polishing scratches (Fig. 6a). After demineralization, the enamel rod structure of the surface layer was clearly observed (Fig. 6b). Inter-prism gaps were seen in demineralized enamel, DW (Fig. 6c), and EBP 0.4 mM (Fig. 6d) and 4.0 mM groups (Fig. 6e). Obscured inter-rod structures were observed in the EBP 7.0 mM group. On the other hand, in the 7.0 mM group, the enamel prism structure was unclear (Fig. 6f). In the longitudinal section, the remaining surface layer and the loss of subsurface structure were seen in all groups (Fig. 7a, b, 7c, 7d 7e, and 7f). In the 7.0 mM group, crystal accumulation was observed in the surface region (Fig. 7f).

## 4. Discussion

In this study, the binding and remineralizing effects of EBPs to demineralized enamel were evaluated. We preliminarily carried out experiments using three peptides identified in the previous study by Mao et al. (2016) [18]. WGNYAYK showed the highest remineralizing effect, and we decided to employ this peptide. The results suggest that EBPs bind to and penetrate demineralized enamel and promote its remineralizing effect. Therefore, the hypothesis proposed in this study was supported. The preliminary data on WGNYAYK as supplementary material is not shown.

Our results showed EBP bound to the enamel surface layer, with an increase in EBP fluorescence intensity. Previous studies reported peptide binding to enamel [13,18]. In this study, we used FITC-labeled EBP to confirm EBP binding to enamel, as the previous study did not visually confirm this [18]. A previous study reported the penetration of a fluorescent dye-labeled protein into longitudinal enamel sections [27]. Longitudinal section images showed FITC localization approximately 20 μm below the surface layer,

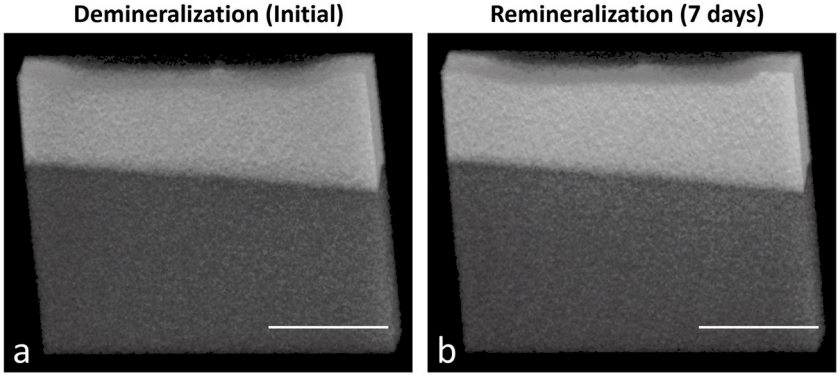


**Fig. 4.** Representative three-dimensional micro-focus X-ray computed tomography (micro-CT) images of the same specimens. X-ray transmission image showing enamel subsurface lesions after demineralization (a).
The radiopacity increased post-remineralization (b). Bars = 1000 μm.

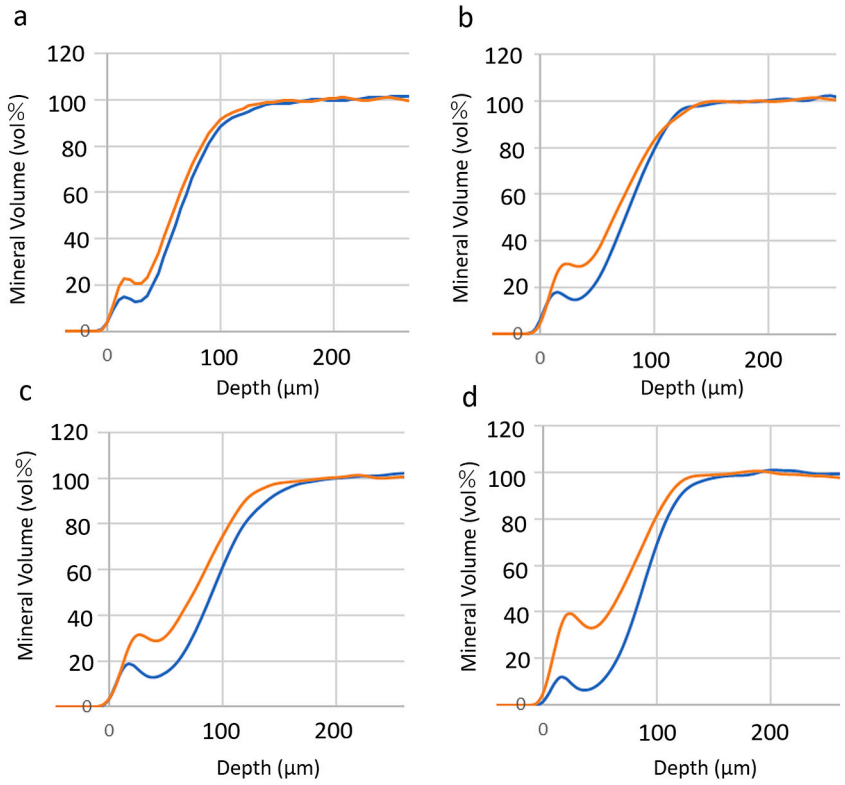


**Fig. 5.** Mean mineral density profiles of representative specimens from experimental groups. Blue line: after demineralization; orange line: after 1 week of remineralization.
Mineral density increased in all groups after 1 week of remineralization (a, b, c, d).
(a) DW, (b) 0.4 mM EBP, (c) 4.0 mM EBP and (d) 7.0 mM EBP.

**Table 1**
Games Howell test of Percentage of Remineralization (%R).

| | mean (%) | | Mean Difference | Standard Error | p-value | 95 % Confidence Interval | |
|---|---|---|---|---|---|---|---|
| | | | | | | Lower Bound | Upper Bound |
| DW | 10.41 | EBP 0.4 mM | −0.807 | 3.008 | 0.993 | −9.73 | 8.116 |
| | | EBP 4.0 mM | −2.214 | 3.073 | 0.887 | −11.345 | 6.918 |
| | | EBP 7.0 mM | −10.706 | 2.726 | 0.008* | −18.723 | −2.688 |
| EBP 0.4 mM | 11.21 | DW | 0.807 | 3.008 | 0.993 | −8.116 | 9.73 |
| | | EBP 4.0 mM | −1.407 | 3.973 | 0.984 | −12.635 | 9.822 |
| | | EBP 7.0 mM | −9.899 | 3.711 | 0.069 | −20.401 | 0.604 |
| EBP 4.0 mM | 12.62 | DW | 2.214 | 3.073 | 0.887 | −6.918 | 11.345 |
| | | EBP 0.4 mM | 1.4067 | 3.973 | 0.984 | −9.822 | 12.635 |
| | | EBP 7.0 mM | −8.492 | 3.764 | 0.147 | −19.151 | 2.167 |
| EBP 7.0 mM | 21.11 | DW | 10.706 | 2.726 | 0.008* | 2.688 | 18.723 |
| | | EBP 0.4 mM | 9.899 | 3.711 | 0.069 | −0.6039 | 20.401 |
| | | EBP 4.0 mM | 8.492 | 3.764 | 0.147 | −2.167 | 19.151 |

The rate of remineralization of EBP 7.0 mM treatment was significantly higher than that of DW treatment ($p = 0.008$). An asterisk in the p-value indicates a significant difference.

implying involvement in mineral uptake. Increasing EBP concentration was associated with an increase in fluorescent intensity of the surface layer and deeper regions, suggesting concentration-dependent binding and permeabilization. The method in our study differs from that in the previous study by Mao et al. [18]. In our study, we used demineralized enamel as in a clinical setting. It is possible that the roughening of the surface layer and disruption of the subsurface structure resulted in more bonding and penetration compare to the sound enamel surface.

Micro-CT is a nondestructive technique to assess mineral content primarily used in mineral density studies and mineral tissue structure, such as bones and teeth [28]. It is useful in evaluating sample remineralization over time [21]. Micro-CT results showed that the most superficial layer remained after 7–9 days of demineralization, while the mineral profile showed a subsurface layer loss, confirming subsurface demineralization. In addition, after remineralization, the subsurface demineralized area radiopacity increased

**Table 2**
Games Howell test of Enamel surface hardness by nano-indentation.

| | mean (N/mm$^2$) | | Mean Difference | Standard Error | p-value | 95 % Confidence Interval | |
|---|---|---|---|---|---|---|---|
| | | | | | | Lower Bound | Upper Bound |
| Sound | 32141.780 | Dem | 28706.363 | 572.777 | <.001* | 26315.841 | 31096.885 |
| | | DW | 25022.224 | 582.907 | <.001* | 22650.654 | 27393.794 |
| | | EBP 0.4 mM | 22720.238 | 634.279 | <.001* | 20357.570 | 25082.906 |
| | | EBP 4.0 mM | 22754.441 | 724.261 | <.001* | 20214.783 | 25294.098 |
| | | EBP 7.0 mM | 18156.085 | 727.572 | <.001* | 15607.226 | 20704.944 |
| Dem | 3435.417 | Sound | −28706.363 | 572.777 | <.001* | −31096.885 | −26315.841 |
| | | DW | −3684.139 | 171.298 | <.001* | −4298.575 | −3069.703 |
| | | EBP 0.4 mM | −5986.125 | 303.105 | <.001* | −7189.015 | −4783.235 |
| | | EBP 4.0 mM | −5951.922 | 462.726 | <.001* | −7861.786 | −4042.059 |
| | | EBP 7.0 mM | −10550.278 | 467.892 | <.001* | −12482.801 | −8617.755 |
| DW | 7119.556 | Sound | −25022.224 | 582.907 | <.001* | −27393.794 | −22650.654 |
| | | Dem | 3684.139 | 171.298 | <.001* | 3069.703 | 4298.575 |
| | | EBP 0.4 mM | −2301.986 | 321.839 | 0.001* | −3505.668 | −1098.304 |
| | | EBP 4.0 mM | −2267.783 | 475.209 | 0.022* | −4160.142 | −375.425 |
| | | EBP 7.0 mM | −6866.139 | 480.240 | <.001* | −8780.996 | −4951.282 |
| EBP 0.4 mM | 9421.542 | Sound | −22720.238 | 634.279 | <.001* | −25082.906 | −20357.570 |
| | | Dem | 5986.125 | 303.105 | <.001* | 4783.235 | 7189.015 |
| | | DW | 2301.986 | 321.839 | 0.001* | 1098.304 | 3505.668 |
| | | EBP 4.0 mM | 34.203 | 536.985 | 1 | −1899.968 | 1968.374 |
| | | EBP 7.0 mM | −4564.153 | 541.443 | <.001* | −6517.590 | −2610.716 |
| EBP 4.0 mM | 9387.339 | Sound | −22754.441 | 724.261 | <.001* | −25294.098 | −20214.783 |
| | | Dem | 5951.922 | 462.726 | <.001* | 4042.059 | 7861.786 |
| | | DW | 2267.783 | 475.209 | 0.022* | 375.425 | 4160.142 |
| | | EBP 0.4 mM | −34.203 | 536.985 | 1 | −1968.374 | 1899.968 |
| | | EBP 4.0 mM | −4598.356 | 644.518 | <.001* | −6837.033 | −2359.678 |
| EBP 7.0 mM | 13985.694 | Sound | −18156.085 | 727.572 | <.001* | −20704.944 | −15607.226 |
| | | Dem | 10550.278 | 467.892 | <.001* | 8617.755 | 12482.801 |
| | | DW | 6866.139 | 480.240 | <.001* | 4951.282 | 8780.996 |
| | | EBP 0.4 mM | 4564.153 | 541.443 | <.001* | 2610.716 | 6517.590 |
| | | EBP 4.0 mM | 4598.356 | 644.518 | <.001* | 2359.678 | 6837.033 |

Unimpaired enamel showed the highest hardness and demineralized enamel showed the lowest hardness.
There were no significant differences among the 0.4 mM and 4.0 mM groups, but the 7.0 mM group showed significantly higher hardness ($p < 0.05$).
An asterisk in the p-value indicates a significant difference.

and %R of EBP 7.0 mM treatment was higher than that of DW treatment. These results indicate that EBP promotes subsurface remineralization. EBP 4.0 mM did not improve mineral recovery because a certain concentration is required before passing through the surface layer and permeating inside. The increased concentration and supersaturation may have allowed EBP to rapidly penetrate the enamel substructure.

While most studies evaluated hard tissue remineralization by measuring mineral content [29,30], it is also important to evaluate mechanical properties to assess the remineralized hard tissue quality [31]. Enamel mechanical properties are strongly related to mineral content [32], and mineral loss causes decreased enamel surface hardness and modulus [33]. Nano-indentation, used in this study, measures indentation depth by displacement, rather than by visually measuring indentation, and is often used to measure demineralized enamel [34]. The results of this study showed that the hardness in demineralized areas was significantly lower than that in unimpaired areas. Compared to immediately after demineralization, each experimental group showed significantly higher hardness values, demonstrating that remineralization restores hardness. In addition, the hardness of all EBP groups was significantly higher than that of the DW group, demonstrating the hardness increase due to the remineralization-promoting effect of EBPs.

In this study, the EBP concentration of up to 7.0 mM demonstrated remineralization, but the concentration dependency was incompletely confirmed. The peptide concentration of 7 mM was the limitation in this study, and the optimal concentration of EBP may be higher. On the other hand, the use of high concentrations or long peptide sequences does not always improve the degree of hardness recovery as shown by Hsu et al. [35]. Further concentration studies are necessary to prove the concentration dependent manner.

Microstructurally sediment-like structures were observed on the surface layer and, in the 7.0 mM EBP group, the interrod structures were obscured, resembling ACP accumulation [18]. The microstructural findings of this study reflected those of Hsu et al., who reported that the 8DSS peptide (derived from the human dentin phosphoprotein) resulted in mineral deposition to the enamel rods and interrod spaces of the demineralized enamel [36]. This study implies that hardness recovery occurs due to surface-layer structure changes.

Protein penetration along with mineral evaluation and microstructural changes in longitudinal sections was reported [13,37]. However, previous studies do not appear to discuss the relationship between the ability of peptides to permeate the tooth and microstructural changes. CLSM data identified FITC-labeled EBP localization approximately 20 μm below the surface layer, but longitudinal SEM sections identified no differences in this area except in the 7.0 mM group. Furthermore, some subsurface crystalline structure recovery was observed, with increased mineral density in the demineralized area approximately 20 μm below the surface for the 7.0 mM group. These results suggest that the ability of EBP to permeate at 7.0 mM promoted mineral uptake and subsurface

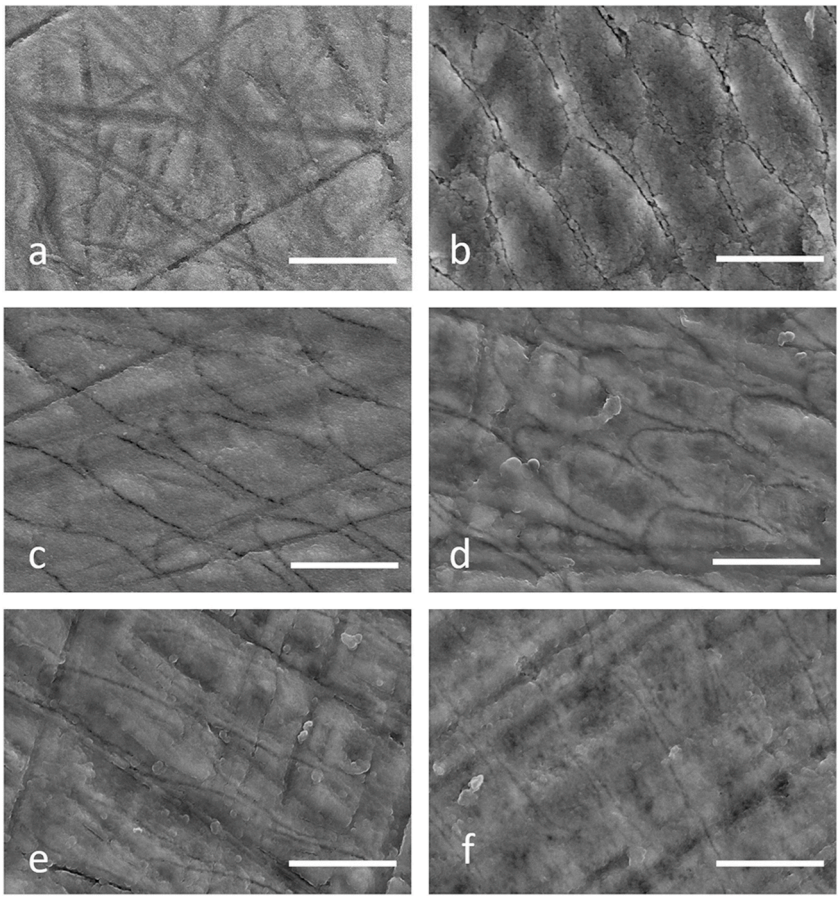


**Fig. 6.** enamel surfaces SEM images.
The surface layer was observed at 7,000x magnification. Unimpaired enamel surface was smooth with polishing scratches (a). Inter-prism gaps were seen in demineralized enamel (b), DW (c), and EBP 0.4 mM (d) and 4.0 mM (e) groups. Obscured inter-rod structures were observed in the EBP 7.0 mM (f) group.
(a) Unimpaired enamel, (b) Demineralization, (c) DW, (d) EBP 0.4 mM, (e) EBP 4.0 mM, (f) EBP 7.0 mM. Bars = 5 μm.

microstructural changes.

The predicted mechanism of EBP remineralization is shown in Fig. 8, where Ding et al. demonstrated amelogenin-derived peptide QP5 binding to the enamel surface, ACP stabilization, hydroxyapatite crystallization control, and promotion of remineralization in caries lesions [38]. EBP is assumed to interact with calcium because there was a high consumption of calcium ions when EBPs were immersed in remineralizing solution [18]. EBP may function similarly, binding to and penetrating demineralized enamel and promoting mineral uptake, thereby generating ACP and crystallizing HAp. We will conduct elemental analysis to analyze newly formed crystals and investigate the characteristics of EBPs to understand the remineralization mechanism of EBP as further studies. Based on the results of the present and further studies, we will consider topical application of EBPs on surface of early enamel caries clinically.

## 5. Conclusion

At higher concentrations, EBP binds to demineralized enamel to promote remineralization under the present experimental conditions.

## Data Availability Statement

Data included in article/supp. material/referenced in article.

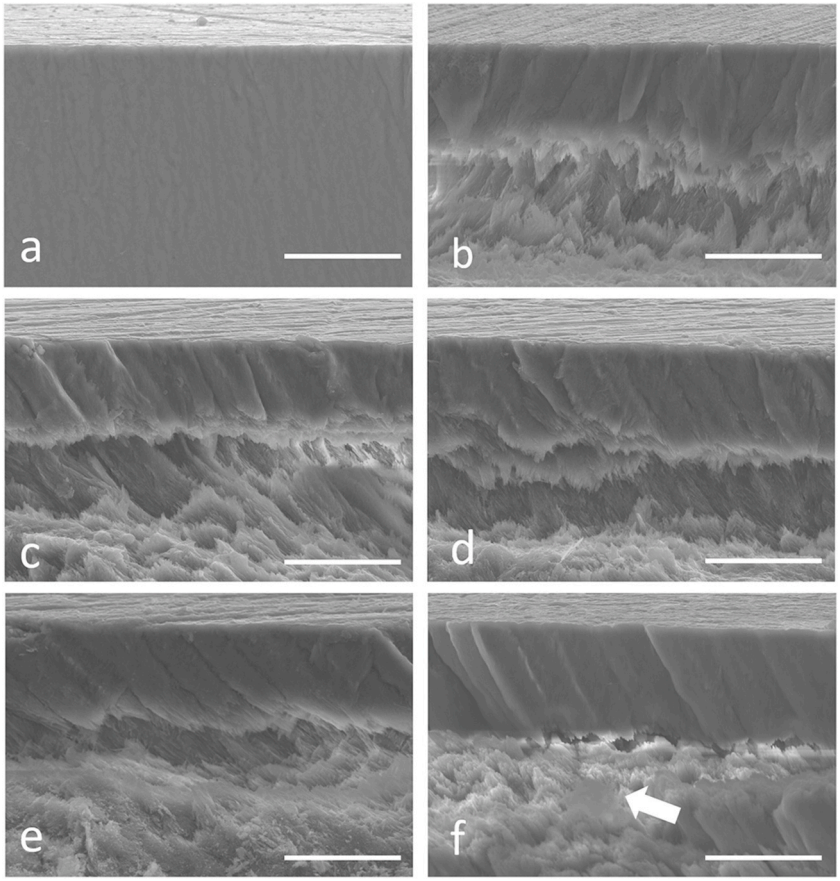


**Fig. 7.** Cross-sectional SEM images of enamel specimens.
The longitudinal section was observed at 2,000x magnification. Unimpaired enamel (a) was smooth, but in the demineralized enamel (b), subsurface lesion-like structures were seen, DW (c), EBP 0.4 mM (d), EBP 4.0 mM (e), and 7.0 mM (f) groups. Note crystal accumulation (white arrow) was seen in subsurface regions of the 7.0 mM group (f).
(a) Unimpaired enamel. (b) Demineralization. (c) DW. (d) EBP 0.4 mM. (e) EBP 4.0 mM. (f) EBP 7.0 mM. Bars = 20 μm.

## Clinical significance

EBPs promote remineralization, supporting EBP-based early treatment of enamel caries.

(*continued on next page*)

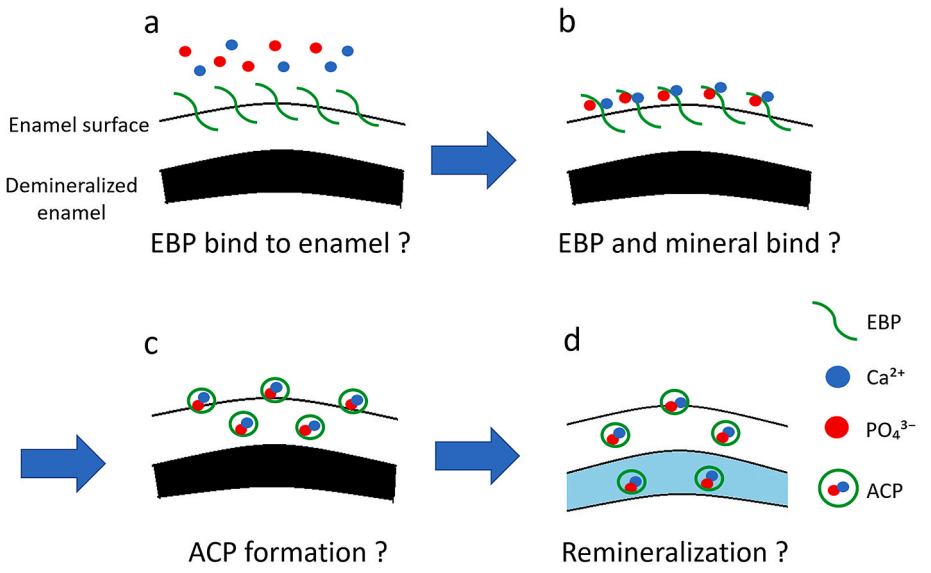


**Fig. 8.** Predicted remineralization mechanism in demineralized enamel after EBP application.
EBP binds to enamel (a), taking up $Ca^{2+}$ and $PO_4^{3-}$ from the remineralization solution (b) and producing ACP (c), which may promote crystallization within the demineralized enamel (d).

(*continued*)

## CRediT authorship contribution statement

**Yoshihito Miyayoshi:** Writing – original draft, Investigation. **Hidenori Hamba:** Visualization, Supervision, Data curation, Conceptualization. **Keiki Nakamura:** Visualization, Resources, Methodology. **Hisako Ishizuka:** Resources, Methodology, Formal analysis. **Takashi Muramatsu:** Writing – review & editing, Supervision, Methodology, Conceptualization.

## Declaration of competing interest

The authors declare that they have no known competing financial interests or personal relationships that could have appeared to influence the work reported in this paper.

## Acknowledgments

We thank Professor Seikou Shintani (Department of Pediatric Dentistry, Tokyo Dental College) for his helpful suggestions.
This work was supported by the Japanese Ministry of Education, Culture, Sports, Science and Technology (Grant-in-Aid No. 21K09960).

## References

[1] C. González-Cabezas, The chemistry of caries: remineralization and demineralization events with direct clinical relevance, Dent Clin North Am 54 (2010) 469–478, https://doi.org/10.1016/j.cden.2010.03.004.

[2] J. Arends, J. Christoffersen, The nature of early caries lesions in enamel, J. Dent. Res. 65 (1986) 2–11, https://doi.org/10.1177/00220345860650010201.
[3] N.J. Cochrane, F. Cai, N.L. Huq, M.F. Burrow, E.C. Reynolds, New approaches to enhanced remineralization of tooth enamel, J. Dent. Res. 89 (2010) 1187–1197, https://doi.org/10.1177/0022034510376046.
[4] J.D. Featherstone, S. Doméjean, Minimal intervention dentistry: part 1. From 'compulsive' restorative dentistry to rational therapeutic strategies, Br. Dent. J. 213 (2012) 441–445, https://doi.org/10.1038/sj.bdj.2012.1007.
[5] J.E. Frencken, Atraumatic restorative treatment and minimal intervention dentistry, Br. Dent. J. 223 (2017) 183–189, https://doi.org/10.1038/sj.bdj.2017.664.
[6] P.R.A. de Oliveira, L. Barreto, M.A. Tostes, Effectiveness of CPP-ACP and fluoride products in tooth remineralization, Int. J. Dent. Hyg. 20 (2022) 635–642, https://doi.org/10.1111/idh.12542.
[7] M. Bossù, M. Saccucci, A. Salucci, G. Giorgio, E. Bruni, D. Uccelletti, M. Sarto, G. Familiari, M. Relucenti, A. Polimeni, Enamel remineralization and repair results of Biomimetic Hydroxyapatite toothpaste on deciduous teeth: an effective option to fluoride toothpaste, J. Nanobiotechnol. 17 (2019) 17, https://doi.org/10.1186/s12951-019-0454-6.
[8] M. Pandya, T.G.H. Diekwisch, Enamel biomimetics-fiction or future of dentistry, Int. J. Oral Sci. 11 (2019) 8, https://doi.org/10.1038/s41368-018-0038-6.
[9] V. Muşat, E.M. Anghel, A. Zaharia, I. Atkinson, O.C. Mocioiu, M. Buşilă, P. Alexandru, A Chitosan-agarose polysaccharide-based hydrogel for biomimetic remineralization of dental enamel, Biomolecules 11 (2021), https://doi.org/10.3390/biom11081137.
[10] Y. Li, Q. Bai, M. Wen, D. Ma, Y. Lin, J. Chu, Recombinant amelogenin peptide TRAP promoting remineralization of early enamel caries: an in vitro study, Front. Physiol. (2023) 14, https://doi.org/10.3389/fphys.2023.1076265.
[11] Y. Cao, M.L. Mei, Q.L. Li, E.C. Lo, C.H. Chu, Enamel prism-like tissue regeneration using enamel matrix derivative, J. Dent. 42 (2014) 1535–1542, https://doi.org/10.1016/j.jdent.2014.08.014.
[12] M. Alkilzy, R.M. Santamaria, J. Schmoeckel, C.H. Splieth, Treatment of carious lesions using self-assembling peptides, Adv. Dent. Res. 29 (2018) 42–47, https://doi.org/10.1177/0022034517737025.
[13] Z. Xiao, K. Que, H. Wang, R. An, Z. Chen, Z. Qiu, M. Lin, J. Song, J. Yang, D. Lu, M. Shen, B. Guan, Y. Wang, X. Deng, X. Yang, Q. Cai, J. Deng, L. Ma, X. Zhang, X. Zhang, Rapid biomimetic remineralization of the demineralized enamel surface using nano-particles of amorphous calcium phosphate guided by chimaeric peptides, Dent. Mater. 33 (2017) 1217–1228, https://doi.org/10.1016/j.dental.2017.07.015.
[14] K. Liang, S. Wang, S. Tao, S. Xiao, H. Zhou, P. Wang, L. Cheng, X. Zhou, M.D. Weir, T.W. Oates, J. Li, H.H.K. Xu, Dental remineralization via poly (amido amine) and restorative materials containing calcium phosphate nanoparticles, Int. J. Oral Sci. 11 (2019) 15, https://doi.org/10.1038/s41368-019-0048-z.
[15] M.J. Romero, S. Nakashima, T. Nikaido, A. Sadr, J. Tagami, In vitro dentine remineralization with a potential salivary phosphoprotein homologue, Arch. Oral Biol. 68 (2016) 35–42, https://doi.org/10.1016/j.archoralbio.2016.03.014.
[16] K.H. Chan, W.H. Lee, S. Zhuo, M. Ni, Harnessing supramolecular peptide nanotechnology in biomedical applications, Int J Nanomedicine 12 (2017) 1171–1182, https://doi.org/10.2147/IJN.S126154.
[17] K. Hashimoto, M. Yoshinari, K. Matsuzaka, K. Shiba, T. Inoue, Identification of peptide motif that binds to the surface of zirconia, Dent. Mater. J. 30 (2011) 935–940, https://doi.org/10.4012/dmj.2011-161.
[18] J. Mao, X. Shi, Y.B. Wu, S.Q. Gong, Identification of specific hydroxyapatite {001} binding heptapeptide by phage display and its nucleation effect, Materials 9 (2016), https://doi.org/10.3390/ma9080700.
[19] H. Ishizuka, H. Hamba, K. Nakamura, Y. Miyayoshi, H. Kumura, T. Muramatsu, Effects of bovine milk osteopontin on in vitro enamel remineralization as a topical application prior to immersion in remineralizing solutions with/without fluoride, Dent. Mater. J. 42 (2023) 140–146, https://doi.org/10.4012/dmj.2022-140.
[20] K. Nakamura, H. Hamba, Y. Miyayoshi, H. Ishizuka, T. Muramatsu, In vitro remineralization of enamel with a solution containing casein and fluoride, Dent. Mater. J. 40 (2021) 1109–1114, https://doi.org/10.4012/dmj.2020-383.
[21] H. Hamba, T. Nikaido, G. Inoue, A. Sadr, J. Tagami, Effects of CPP-ACP with sodium fluoride on inhibition of bovine enamel demineralization: a quantitative assessment using micro-computed tomography, J. Dent. 39 (2011) 405–413, https://doi.org/10.1016/j.jdent.2011.03.005.
[22] M. Fan, M. Zhang, H.H.K. Xu, S. Tao, Z. Yu, J. Yang, H. Yuan, X. Zhou, K. Liang, J. Li, Remineralization effectiveness of the PAMAM dendrimer with different terminal groups on artificial initial enamel caries in vitro, Dent. Mater. 36 (2020) 210–220, https://doi.org/10.1016/j.dental.2019.11.015.
[23] X. Lv, Y. Yang, S. Han, D. Li, H. Tu, W. Li, X. Zhou, L. Zhang, Potential of an amelogenin based peptide in promoting reminerlization of initial enamel caries, Arch. Oral Biol. 60 (2015) 1482–1487, https://doi.org/10.1016/j.archoralbio.2015.07.010.
[24] R.J. Jennings, A method for comparing beam-hardening filter materials for diagnostic radiology, Med. Phys. 15 (1988) 588–599, https://doi.org/10.1118/1.596210.
[25] K.W. Zan, K. Nakamura, H. Hamba, A. Sadr, T. Nikaido, J. Tagami, Micro-computed tomography assessment of root dentin around fluoride-releasing restorations after demineralization/remineralization, Eur. J. Oral Sci. 126 (2018) 390–399, https://doi.org/10.1111/eos.12558.
[26] H.Y. Chung, C.C. Li, Microstructure and nanomechanical properties of enamel remineralized with asparagine-serine-serine peptide, Mater Sci Eng C Mater Biol Appl 33 (2013) 969–973, https://doi.org/10.1016/j.msec.2012.11.031.
[27] J.R. Fernando, P. Shen, G.D. Walker, Y. Yuan, D.P. Stanton, C. Reynolds, E.C. Reynolds, Effects of bovine serum albumin and high pH pre-treatment on the remineralisation of enamel subsurface lesions in vitro, Caries Res. 54 (2020) 36–42, https://doi.org/10.1159/000502337.
[28] S.R. Stock, J. Barss, T. Dahl, A. Veis, J.D. Almer, X-ray absorption microtomography (microCT) and small beam diffraction mapping of sea urchin teeth, J. Struct. Biol. 139 (2002) 1–12, https://doi.org/10.1016/s1047-8477(02)00500-2.
[29] A.B. Neves, T.G. Bergstrom, A. Fonseca-Gonçalves, T.M.P. Dos Santos, R.T. Lopes, A. de Almeida Neves, Mineral density changes in bovine carious dentin after treatment with bioactive dental cements: a comparative micro-CT study, Clin. Oral Invest. 23 (2019) 1865–1870, https://doi.org/10.1007/s00784-018-2644-2.
[30] P. Körner, J.A. Schleich, D.B. Wiedemeier, T. Attin, F.J. Wegehaupt, Effects of additional use of bioactive glasses or a hydroxyapatite toothpaste on remineralization of artificial lesions in vitro, Caries Res. 54 (2020) 336–342, https://doi.org/10.1159/000510180.
[31] L.E. Bertassoni, S. Habelitz, S.J. Marshall, G.W. Marshall, Mechanical recovery of dentin following remineralization in vitro–an indentation study, J. Biomech. 44 (2011) 176–181, https://doi.org/10.1016/j.jbiomech.2010.09.005.
[32] R. Alkattan, F. Lippert, Q. Tang, G.J. Eckert, M. Ando, The influence of hardness and chemical composition on enamel demineralization and subsequent remineralization, J. Dent. 75 (2018) 34–40, https://doi.org/10.1016/j.jdent.2018.05.002.
[33] C.P. Wang, S.B. Huang, Y. Liu, J.Y. Li, H.Y. Yu, The CPP-ACP relieved enamel erosion from a carbonated soft beverage: an in vitro AFM and XRD study, Arch. Oral Biol. 59 (2014) 277–282, https://doi.org/10.1016/j.archoralbio.2013.11.018.
[34] M.E. Dickinson, K.V. Wolf, A.B. Mann, Nanomechanical and chemical characterization of incipient in vitro carious lesions in human dental enamel, Arch. Oral Biol. 52 (2007) 753–760, https://doi.org/10.1016/j.archoralbio.2007.02.007.
[35] H.Y. Chung, K.C. Huang, Effects of peptide concentration on remineralization of eroded enamel, J. Mech. Behav. Biomed. Mater. 28 (2013) 213–221, https://doi.org/10.1016/j.jmbbm.2013.08.004.
[36] C.C. Hsu, H.Y. Chung, J.M. Yang, W. Shi, B. Wu, Influence of 8DSS peptide on nano-mechanical behavior of human enamel, J. Dent. Res. 90 (2011) 88–92, https://doi.org/10.1177/0022034510381904.
[37] F. Hua, J. Yan, S. Zhao, H. Yang, H. He, In vitro remineralization of enamel white spot lesions with a carrier-based amorphous calcium phosphate delivery system, Clin. Oral Invest. 24 (2020) 2079–2089, https://doi.org/10.1007/s00784-019-03073-x.
[38] L. Ding, S. Han, K. Wang, S. Zheng, W. Zheng, X. Peng, Y. Niu, W. Li, L. Zhang, Remineralization of enamel caries by an amelogenin-derived peptide and fluoride in vitro, Regen Biomater 7 (2020) 283–292, https://doi.org/10.1093/rb/rbaa003.